FULL PAPER

Dalton
www.rsc.org/dalton

A rare structural characterisation of the phosphomolybdate lacunary anion, $[PMo_{11}O_{39}]^{7-}$. Crystal structures of the Ln(III) complexes, $(NH_4)_{11}[Ln(PMo_{11}O_{39})_2]\cdot 16H_2O$ (Ln = Ce^{III}, Sm^{III}, Dy^{III} or Lu^{III})†

Andrew J. Gaunt,[a] Iain May,*[a] Mark J. Sarsfield,[a] David Collison,[b] Madeleine Helliwell[b] and Iain S. Denniss[c]

[a] *Centre for Radiochemistry Research, Department of Chemistry, The University of Manchester, Manchester, UK M13 9PL. E-mail: Iain.May@man.ac.uk*

[b] *Department of Chemistry, The University of Manchester, Manchester, UK M13 9PL*

[c] *Research and Technology, BNFL, Sellafield, Seascale, Cumbria, UK CA20 1PG*

Received 20th February 2003, Accepted 23rd May 2003
First published as an Advance Article on the web 10th June 2003

The syntheses and the crystal structures of $(NH_4)_{11}[Ln^{III}(PMo_{11}O_{39})_2]\cdot 16H_2O$ (Ln^{III} = Ce (**1**), Sm (**2**), Dy (**3**) or Lu (**4**)) are reported in which an Ln^{III} cation is sandwiched between two 'lacunary' $[PMo_{11}O_{39}]^{7-}$ anions to give a complex with eight oxygen atoms coordinated to the lanthanide centre in a twisted square antiprismatic geometry. This analogous series of complexes represents only the second time that the $[PMo_{11}O_{39}]^{7-}$ anion has been fully crystallographically characterised. All four compounds are synthesised in high yield and characterised by a range of physical and spectroscopic techniques. ^{31}P NMR, Raman and UV/Vis/nIR spectroscopies give a clear indication that the $[Ln^{III}(PMo_{11}O_{39})_2]^{11-}$ anion is also stable in solution. As Ln^{III} contracts across the lanthanide series the Ln–O bond distances decrease and the splitting of the ν_{P-O} vibrational mode within the $[PMo_{11}O_{39}]^{7-}$ unit increases. The relative stability of this species in solution may have importance in elucidating the speciation of Ln(III) and An(III) cations in nuclear waste solutions where phosphopolymolybdate anions are known to form.

Introduction

Polyoxometalate anions are extensively studied because of their application in catalysis, biochemistry, analytical chemistry and separation science.[1] We are interested in investigating heteropolymolybdate chemistry in acidic aqueous nuclear waste solutions generated from fuel reprocessing operations. In many radioactive waste solutions phosphates are present and the Keggin anion, $[\alpha\text{-}PMo_{12}O_{40}]^{3-}$, dominates molybdenum speciation in acidic phosphorous containing waste.[1,2] A range of Keggin anions incorporating many heteroatoms have been previously structurally and spectroscopically characterised.[3] As the acidity is lowered the Keggin anion can lose a {Mo–O} unit resulting in the formation of the lacunary anion, $[\alpha\text{-}PMo_{11}O_{39}]^{7-}$, which has unsaturated oxygen atoms available for coordination to other metal ions.[4–7] Previous attempts to crystallographically characterise complexes containing this group have failed due to disorder in the $[PMo_{11}O_{39}]^{7-}$ cluster, although we have recently structurally characterised a Zr^{4+} complex that is coordinated to both $[PMo_{11}O_{39}]^{7-}$ and $[PMo_{12}O_{40}]^{3-}$ anions.[8] The related lacunary, $[PW_{11}O_{39}]^{7-}$, has also recently been structurally characterised in $[(CH_3)_4N]_4Na_2H[\alpha\text{-}PW_{11}O_{39}]\cdot 8H_2O$, in which one of the two associated Na^+ cations sits in the space left by the loss of the {W–O} unit and interacts with a terminal O atom of another $[\alpha\text{-}PW_{11}O_{39}]^{7-}$ anion forming a chain structure.[9] We are currently studying the interaction of $[PMo_{11}O_{39}]^{7-}$ with a range of metal ions that are present in significant quantities in nuclear waste solutions. Of particular interest is the interaction of this lacunary species with the trivalent f-element cations, which are known to form a range of stable complexes with polyoxometalates.[10] We are initially focussing on the non-radioactive Ln^{III} ions, which are present in comparatively high concentrations in many nuclear waste solutions and which have recently been shown to form a range of structurally distinct complexes with lacunary heteropolyoxotungstate anions.[11]

In a solution containing dissolved $H_3PMo_{12}O_{40}\cdot xH_2O$ (0.1 M, pH = 1), $[PMo_{12}O_{40}]^{3-}$ is the major species present, as shown by ^{31}P NMR spectroscopy. Raising the pH to 4.3 affords $[PMo_{11}O_{39}]^{7-}$ as the predominant species.[4–6] The lacunary anion can be precipitated from solution as a $[NBu_4]^+$ salt and crystallised from MeCN in high yield.[6,7] This lacunary phosphomolybdate anion is known to react with Ln^{III} ions yielding $[Ln^{III}(PMo_{11}O_{39})_2]^{11-}$, which are proposed to contain two $[PMo_{11}O_{39}]^{7-}$ groups sandwiching an Ln^{III} anion, although none of the complexes formed have previously been fully structurally characterised.[12] The corresponding lanthanide complexes of the tungsten analogues, $[Ln^{III}(PW_{11}O_{39})_2]^{11-}$ are more stable and have been prepared and characterised by other workers, although again no complexes have been fully structurally characterised.[1] The only additional reported single crystal X-ray studies of lacunary heteropolymolybdate anions refers to the compounds $K_7H_6[Nd(GeMo_{11}O_{39})_2]\cdot 27H_2O$,[13] and $[Dy(SiMo_{11}O_{39})_2]^{13-}$ in $K_{10}H_3[Dy(SiMo_{11}O_{39})_2]\cdot 29H_2O$,[14] $K_{11}H_2[Dy(SiMo_{11}O_{39})_2]\cdot 29H_2O$[15] and $K_{10}H_3[Dy(SiMo_{11}O_{39})_2]\cdot 20H_2O$.[16] Herein we present the first single crystal X-ray diffraction studies of Ln^{III} coordinated to the $[PMo_{11}O_{39}]^{7-}$ anion in the sandwich complexes $(NH_4)_{11}[Ln^{III}(PMo_{11}O_{39})_2]\cdot 16H_2O$ (Ln = Ce (**1**), Sm (**2**) Dy (**3**) and Lu (**4**)).

Results and discussion

Syntheses and bulk characterisation

Synthesis of the title compounds involved dissolution of $H_3PMo_{12}O_{40}\cdot xH_2O$ in H_2O followed by adjustment of the pH to 4.3 by the addition of Li_2CO_3 to form the $[PMo_{11}O_{39}]^{7-}$ anion. Introduction of an Ln^{III} salt to the solution forms $[Ln^{III}(PMo_{11}O_{39})_2]^{11-}$ which, after the addition of NH_4Cl, a few drops of EtOH or CH_3CN and storage at 5 °C for several days, yields brown plates for Ln = Ce^{III} and yellow plates for Ln = Sm^{III}, Dy^{III} and Lu^{III}, characterised as $(NH_4)_{11}[Ln^{III}(PMo_{11}O_{39})_2]\cdot 16H_2O$ by X-ray diffraction. Powder XRD was used to confirm that the bulk material was identical to the material used for single crystal XRD. The lacunary anion itself can also be

† Electronic supplementary information (ESI) available: IR, Raman and UV/vis/nIR spectra and TGA curves for **1**–**4**. See http://www.rsc.org/suppdata/dt/b3/b301995k/

DOI: 10.1039/b301995k

Table 1 Selected bond distances (Å) for $(NH_4)_{11}[Ln^{III}(PMo_{11}O_{39})_2]\cdot 16H_2O$, Ln = Ce^{III}, Sm^{III}, Dy^{III} and Lu^{III}

	Distance/Å			
Bond Ln^{III} =	Ce (**1**)	Sm (**2**)	Dy (**3**)	Lu (**4**)
Ln1–O1	2.486(3)	2.423(9)	2.379(4)	2.325(4)
Ln1–O2	2.446(3)	2.405(10)	2.352(4)	2.308(4)
Ln1–O3	2.489(3)	2.436(9)	2.389(4)	2.341(4)
Ln1–O4	2.453(3)	2.403(9)	2.357(4)	2.316(4)
Average short Ln–O	2.449	2.404	2.354	2.312
Average long Ln–O	2.487	2.429	2.384	2.333
Mo1–O1	1.756(3)	1.784(9)	1.755(3)	1.755(4)
Mo2–O2	1.750(3)	1.757(10)	1.748(4)	1.742(4)
Mo3–O3	1.744(3)	1.744(9)	1.740(4)	1.735(4)
Mo4–O4	1.737(3)	1.742(9)	1.740(4)	1.737(5)
P–O5	1.524(3)	1.537(10)	1.523(4)	1.522(4)
P–O20	1.546(3)	1.553(9)	1.538(3)	1.540(3)
P–O24	1.541(3)	1.544(9)	1.543(4)	1.544(4)
P–O28	1.546(3)	1.543(9)	1.543(3)	1.540(3)

crystallised from solution by the addition of $[NBu_4]Cl$ (instead of the Ln^{III} salt), followed by recrystallisation from MeCN.[6,7] Spectroscopic characterisation of the crystalline product is consistent with the formation of the $[PMo_{11}O_{39}]^{7-}$ anion, however our attempts at an X-ray structural determination have not yet succeeded because of disorder in the crystal.

TGA curves for **1**–**4** were recorded in the presence of N_2 gas and show four significant weight losses in the 25–1000 °C temperature range (see ESI † for the TGA curves). The first step, in the region 25–100 °C accounts for approximately 5–7.3% of the weight loss and can be attributed to the loss of water molecules in the samples present as either moisture or weakly bound lattice molecules. From the X-ray structural data, 16 H_2O molecules have been assigned to compounds **1**–**4**, and it would appear that 8 of these are weakly bound lattice molecules. The second step, between 200 and 300 °C accounts for 3.5–4% of the sample weight loss and is attributed in the TGA curves to the loss of 8 more strongly held water molecules of crystallisation. Between 350–450 °C an additional 4–5% weight loss is observed, which can be attributed to the decomposition of 11 NH_4^+ cations to NH_3. Further weight loss above 700 °C is probably due to further reductive decomposition and the formation of Mo metal. From the TGA data the water content of **1**–**4** were calculated and the value used when quoting the formula of the bulk product. The water content values are larger than observed in the single crystals from the single crystal X-ray diffraction study due to additional moisture in the bulk product. These values were also used to calculate expected elemental percentages for elemental analysis, which are in reasonably good agreement with the experimental values obtained.

Single crystal X-ray diffraction

Single crystal X-ray analysis of **1**–**4** shows all four compounds to be isomorphous, with monoclinic unit cells and space group C2/c. Selected bond lengths and angles are given in Tables 1 and 2, respectively. All the compounds contain an Ln^{III} cation sandwiched between two 'lacunary' $[PMo_{11}O_{39}]^{7-}$ anions in which the trivalent lanthanide has a coordination number of eight and occupies square antiprismatic geometry (Fig. 1).[17] Each lacunary $[PMo_{11}O_{39}]^{7-}$ anion coordinates its four unsaturated oxygen atoms to the Ln^{III} metal centre. The square-antiprismatic geometry is confirmed by applying the criteria for eight-coordinate structure-type determination outlined by Haigh where a gap of more than 20° between the 16th and 17th O–Ln–O angles, evident in all four complexes, denotes square antiprismatic coordination.[18] For example, in **4** the 16th lowest O–Lu–O angle is 84.29(15)° and the 17th lowest O–Lu–O angle is 115.44(15)°; a gap of 31.2°. The structure is comparable to $[Nd(GeMo_{11}O_{39})_2]^{11-}$ and $[Dy(SiMo_{11}O_{39})_2]^{11-}$ anions, which have similar geometry.[13–15] Predictably, the Ln–O bond distances decrease across the lanthanide series because of the stronger degree of interaction between the lanthanide and the unsaturated oxygen atoms as the ionic radius of the Ln^{III} ion decreases (lanthanide contraction). The average Dy–O bond distance in **3** is 2.369 Å, which is comparable to the average Dy–O bond distance in $K_{10}H_3[Dy(SiMo_{11}O_{39})_2]\cdot 29H_2O$ of 2.372 Å.[14]

On closer inspection two types of Ln–O bonds can be distinguished by their lengths for both **1** and **3**. There are four 'long' Ln–O bonds and four 'short' ones. This is a feature present in other structurally determined lacunary-lanthanide complexes.[13–16] The average short and long Ln–O bonds in complex **3** are 2.355 and 2.384 Å, respectively compared to 2.360 and 2.383 Å for $K_{10}H_3[Dy(SiMo_{11}O_{39})_2]\cdot 29H_2O$.[14] For the Sm (**2**) and Lu (**4**) complexes there is less clear distinction between the

Table 2 Unique O–Ln–O bond angles in $(NH_4)_{11}[Ln^{III}(PMo_{11}O_{39})_2]\cdot 16H_2O$, Ln = Ce^{III}, Sm^{III}, Dy^{III} and Lu^{III}, The atoms marked by an asterisk (*) are generated by an inversion centre at Ln^{III}

	Angle/°			
Bond Ln^{III} =	Ce (**1**)	Sm (**2**)	Dy (**3**)	Lu (**4**)
O1–Ln–O3	73.56(11)	73.5(3)	73.71(12)	73.66(15)
O1–Ln–O3*	72.25(10)	71.5(3)	72.00(12)	72.03(15)
O1*–Ln–O1	133.24(15)	132.4(5)	133.70(17)	133.9(2)
O2–Ln–O3	74.68(11)	75.0(3)	75.13(13)	75.32(16)
O2–Ln–O4	69.27(11)	70.0(3)	70.02(12)	70.18(15)
O2–Ln–O1*	85.41(11)	84.1(3)	84.51(12)	84.29(15)
O2*–Ln–O2	129.23(15)	129.9(4)	129.98(17)	130.2(2)
O2*–Ln–O3	154.07(11)	152.9(3)	152.94(12)	152.55(15)
O2*–Ln–O4	72.36(11)	72.2(3)	72.20(12)	72.21(15)
O2*–Ln–O1*	114.85(10)	116.3(3)	115.35(12)	115.45(15)
O3–Ln–O3*	81.41(15)	83.5(4)	82.87(18)	82.4(2)
O4–Ln–O1	75.53(11)	75.9(3)	75.25(13)	75.16(16)
O4–Ln–O3	115.26(11)	115.3(3)	115.92(3)	116.04(15)
O4–Ln–O1*	149.09(10)	149.2(3)	148.93(12)	148.87(15)
O4–Ln–O4*	79.95(16)	80.3(4)	80.09(18)	80.1(2)
O4*–Ln–O3	135.12(11)	135.5(3)	135.30(12)	135.47(15)

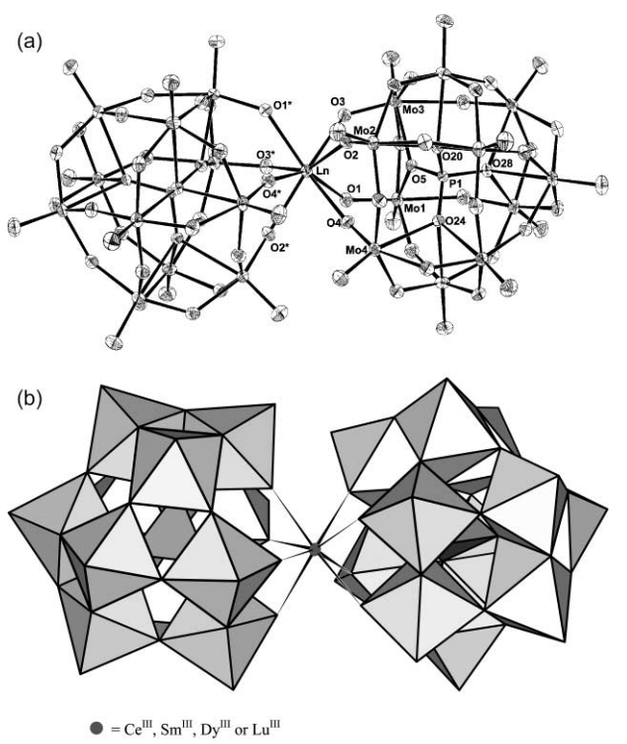

Fig. 1 The structure of the anion of $(NH_4)_{11}[Ln^{III}(\alpha\text{-}PMo_{11}O_{39})_2]\cdot 16H_2O$.[17] (a) ORTEP representation where Ln = Ce^{III} (**1**), Sm^{III} (**2**), Dy^{III} (**3**) or Lu^{III} (**4**). (b) Polyhedral representation. Mo atoms are at the centre of each octahedron, P at the centre of the tetrahedron and the corners of the polyhedra represent O atoms.

Table 3 Selected assignable infrared stretching frequencies for **1**–**4** and $(n\text{-}Bu_4N)_4H_3PMo_{11}O_{39}$ obtained in the solid state (with solution state measurements in parentheses, where recorded)

Compound	Stretching frequency assignment/cm^{-1}			
	P–O	Δ(P–O)	$Mo–O_{terminal}$	$Mo–O–Mo_{corner\text{-}shared}$ and $Mo–O–Mo_{edge\text{-}shared}$
$(n\text{-}Bu_4N)_4H_3PMo_{11}O_{39}$	1068, 1043	25	933	883, 854, 820, 795, 779, 727
1 (Ce^{III})	1072, 1034	38	936	884, 852, 774
	(1070, 1032)	(38)	(936)	
2 (Sm^{III})	1078, 1034	44	936	866, 819
	(1077, 1034)	(43)	(937)	
3 (Dy^{III})	1082, 1035	45	937	887, 781
	(1081, 1036)	(45)	(938)	
4 (Lu^{III})	1088, 1036	52	934	870, 824, 725
	(1089, 1037)	(52)	(939)	

long and short Ln–O bonds. For complex **2** this is because of the poorer quality of data refinement arising from crystal twinning.

The origin of the long and short Ln–O bonds is rationalised by consideration of the parent Keggin structure, $[XMo_{12}O_{40}]^{n-}$ where X = a range of heteroatoms, in which four types of O atoms can be distinguished, evident in the crystal structure of $Na_4[GeMo_{12}O_{40}]\cdot 8H_2O$[19] and for the $[PMo_{12}O_{40}]^{3-}$ anion in $[(CH_2OH)_3CNH_3]_3[PMo_{12}O_{40}]\cdot 5H_2O$.[20] The four distinctive oxygen environments are: (i) O singly bonded to one Mo atom (terminal Mo=O bond), (ii) O bonded to the heteroatom and one Mo atom, (III) O coordinated to two Mo atoms through edge-shared Mo octahedra ('short' Mo–O bonds, 1.79–1.86 Å), (iv) O coordinated to two Mo atoms through corner-shared Mo octahedra ('long' Mo–O bonds, 1.99–2.08 Å).[19] Removal of one terminal {Mo–O} unit from a Keggin anion gives the monovacant lacunary species with two oxygen atoms available for bonding to the lanthanide having short Mo–O bonds and two having long Mo–O bonds. This difference is translated into the Ln–O bond distances in the sandwich $[Ln^{III}(PMo_{11}O_{39})]^{11-}$ complexes with the two long Ln–O bonds having oxygen atoms originating from edge-shared Mo octahedra and the two short Ln–O bonds having oxygen atoms originating from corner-shared Mo octahedra, although the difference in bond lengths is an order of magnitude lower than the ~0.2 Å observed for $[XMo_{12}O_{40}]^{n-}$ (X = P or Ge) anions.[19,20] The 'long' and 'short' Ln–O bonds cause a distortion in the square-antiprismatic geometry and this distortion can be related to with the dihedral angle between diagonals of opposite faces calculated to be *ca.* 34° in all four complexes. It should be noted that there are no distinctive long and short Mo–O bond lengths for the oxygen atoms also bound to the Ln(III) centres for any of the four lancunary complexes reported here. This feature is only observed in single crystal structures of Keggin anions when crystallised in a low symmetry space group.[19,20]

Comparing the P–O bond distance in the Keggin anion, $[PMo_{12}O_{40}]^{3-}$, in $H_3PMo_{12}O_{40}\cdot ca.30H_2O$ (1.499(11) Å)[21] to those in **1**–**4** show they are longer in the four lacunary complexes. The P–O(5) bond, which is closest to, and points towards, the lanthanide centre in each complex, is shorter than the other three P–O bonds that make up the central tetrahedron. The closest Mo–O bonds to the lanthanide display very little variation in bond distance upon replacement of one rare earth element with another. There is also no appreciable effect on the P–O bond distances with varying lanthanide, which is unsurprising when considering the remoteness of the P–O bond from the lanthanide centre, although the magnitude of the splitting of the P–O stretching vibration does increase going across the series (see the following spectroscopic study).

Spectroscopic characterisation

Infrared spectra were recorded on **1**–**4** in both the solid state, as KBr discs, and in aqueous solution, using ATR-IR, with major bands assigned in Table 3 (see also ESI † for spectra). Although the aqueous solution spectra are of poorer quality it can be seen that the spectra in both phases are similar, providing evidence to support the existence of the $[Ln^{III}(PMo_{11}O_{39})_2]^{11-}$ anion in solution. The infrared spectra of all four complexes (see Fig. 2) show a splitting of the P–O stretching band, indicative of the lacunary anion and originating from the removal of the T_d symmetry that accompanies the loss of an {Mo–O} unit from $[PMo_{12}O_{40}]^{3-}$. The size of the splitting increases from 25 cm^{-1} in the uncomplexed lacunary anion, $(n\text{-}Bu_4N)_4H_3[PMo_{11}O_{39}]$, to 38 cm^{-1} in **1**; probably because of the increased distortion from T_d symmetry on coordination. The size of the splitting increases across the four Ln^{III} complexes, from 38 cm^{-1} (Ce^{III}), to 44 cm^{-1} (Sm^{III}), 45 cm^{-1} (Dy^{III}), and finally 52 cm^{-1} (Lu^{III}), perhaps due to the increased interaction between $[PMo_{11}O_{39}]^{7-}$ and the lanthanide ion as you go across the series. The characteristic Mo–O (terminal) band is observed in the range 934–939 cm^{-1} for **1**–**4** and several overlapping bands between 900–700 cm^{-1} can be assigned to Mo–O–Mo (corner shared) and Mo–O–Mo (edge shared) stretching modes, although identifying separate peaks is not always possible in this lower energy region. There is no evidence for a Ln–O stretching vibration in the far-infrared region, probably because of the predominantly ionic character of the interaction between the lacunary anion and the central Ln^{III} cation.

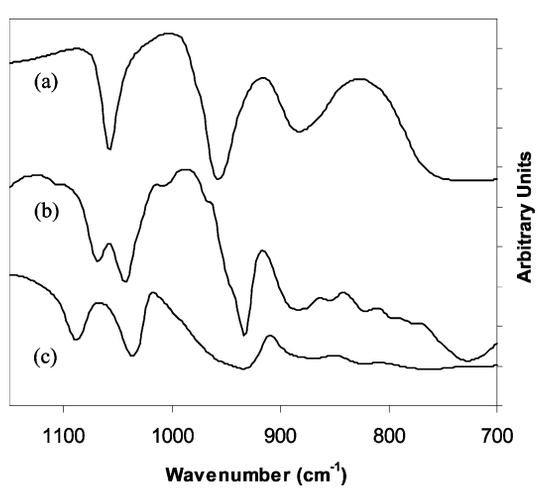

Fig. 2 Infrared spectra of $H_3PMo_{12}O_{40}$ (a), $(n\text{-}Bu_4N)_4H_3PMo_{11}O_{39}$ (b) and **4** (c) as KBr discs. The ν_{P-O} stretching region is between 1000–1100 cm^{-1}.

The Raman spectra of **1**–**4** show only one major band in the region 965–967 cm^{-1}, which can be assigned to the O–Mo–O symmetric stretch with shoulders at 947 and 930 cm^{-1}, assigned to the associated asymmetric stretching modes. The aqueous solution spectra are almost identical, except for the lower resolution of the peaks. As for the molybdenum–oxygen stretching vibrations observed in the IR, there is no variation in peak position in **1**–**4** (see ESI † for spectra).

The ^{31}P NMR spectra of **1**–**4** in aqueous solution contain one major peak attributed to the $[Ln^{III}(PMo_{11}O_{39})_2]^{11-}$ anion. Uncoordinated $[PMo_{11}O_{39}]^{7-}$ is observed at −0.8 ppm, with a slight variation in peak position depending on concentration and solution pH. For compounds **1**–**3** a wide range of ^{31}P chemical shift values are identified (Ce^{III} −5.58 ppm, Sm^{III} −4.10 ppm and Dy^{III} −69.70 ppm) with increased linewidth compared to the ^{31}P signal for uncomplexed $[PMo_{11}O_{39}]^{7-}$. This may be expected for complexation of the lacunary anion to a paramagnetic centre. The largest difference in chemical shift is observed for the most paramagnetic lanthanide complex (calculated μ_{eff} for Dy^{III} = 10.65 μ_B). In contrast, a much sharper peak is observed for the diamagnetic Lu^{III} complex (**4**) with the peak shifted to only −2.58 ppm.

The UV/vis/nIR spectra were recorded for **1**–**4** in aqueous solution and in the solid state (diffuse reflectance spectra). Two types of feature were observed in the spectra; high energy LMCT bands associated with the polyoxometalate (O⟶Mo) and lower intensity bands arising from Laporte forbidden f–f transitions within the Sm^{III} and Dy^{III} cations. The higher energy f–f transitions were masked by LMCT charge transfer bands. The solution and solid-state spectra for individual complexes are similar with variation in f–f transition peak intensities going from solution to solid state attributed to lowered symmetry in the solid state (see ESI †for spectra).

Experimental

General

All chemicals were reagent grade, obtained commercially and used without purification. Water was purified by distillation and $(n\text{-}Bu_4N)_4H_3[PMo_{11}O_{39}]$ was prepared according to the literature method.[6,7] IR spectra were obtained from a Bruker Equinox 55/Bruker FRA 106/5 spectrometer with a coherent 500 mW Laser as either KBr pellets for solid-state measurements or as ~0.05 mol L^{-1} aqueous solutions using an ATR Golden Gate attachment. Raman spectra were recorded on the same instrument in both the solid state (20 mg samples) and in aqueous solution (~0.05 mol L^{-1}). The IR and Raman spectra were recorded with a resolution of 2 cm^{-1}. Elemental analysis was performed on a Carlo ERBA Instruments CHNS-O EA1108 Elemental Analyser for C, H and N and by a Fisons Horizon Elemental Analysis ICP-OED spectrometer for Mo and for Ln. ^{31}P NMR spectra were recorded in D_2O on a Bruker Avance 400 MHz spectrometer in 5 mm diameter NMR sample tubes and referenced against H_3PO_4 (85%) Thermogravimetric analaysis (TGA) was recorded on a Metler Toledo TGA/SDTA 851^e analyser with a heating rate of 5 °C min^{-1} under a continuous stream of nitrogen. UV/vis/nIR absorption solution spectra were recorded on a Cary Varian 500 Scan UV-Vis-NIR spectrophotometer at a scan rate of 50 nm min^{-1} with H_2O used for background subtraction. Diffuse reflectance solid-state measurements were recorded on an Ocean Optics SD2000 spectrometer with a fibre optic probe using a Deuterium–Halogen DH-200 light source with $BaSO_4$ used for background subtraction.

Syntheses

$(NH_4)_{11}[Ce^{III}(PMo_{11}O_{39})_2]\cdot xH_2O$ (1). This was isolated as follows: $H_3PMo_{12}O_{40}$ (4.68 g, 2.00 mmol) (78%) (remainder moisture) was dissolved in H_2O (20 cm^3) with stirring and the pH was adjusted up to 4.3 by addition of Li_2CO_3. $Ce^{III}(NO_3)_3\cdot 6H_2O$ (0.434 g, 1.00 mmol) was added directly to the solution resulting in an immediate colour change from yellow–green to dark brown. The pH of the solution was re-adjusted back up to 4.3 by further addition of Li_2CO_3 solid. $(NH_4)Cl$ (2.94 g, 54.9 mmol) was added and the solution left stirring for 1 h. A few drops of EtOH were added to a portion of the solution (3 cm^3) until it was no longer immediately miscible with shaking. The solution was kept at 5 °C for a few days yielding brown plate crystals (0.17 g), one of which was used for single crystal XRD. To the remainder of the solution EtOH was added dropwise with shaking until it was no longer immediately miscible and the solution stored at 5 °C for several days giving a dark brown crystalline solid (3.12 g, 76%), which was filtered, washed with EtOH and air-dried. Powder XRD was used to confirm that the bulk material was identical to the material used for single crystal XRD. Elemental analysis: calc. (found) (%) for $(NH_4)_{11}[Ce^{III}(PMo_{11}O_{39})_2]\cdot 20.7H_2O$: H 2.07 (1.77), N 3.73 (3.63), P 1.50 (1.66), Ce 3.39 (3.29), Mo 54.08 (54.66).

$(NH_4)_{11}[Sm^{III}(PMo_{11}O_{39})_2]\cdot xH_2O$ (2). This was synthesized as for **1** using $Sm(NO_3)_3\cdot 6H_2O$ (0.445 g, 1.00 mmol) to give a Sm : P stoichiometry of 1 : 2. Instead of adding EtOH a few drops of CH_3CN were added to a portion (3 cm^3) of the solution and this was stored at 5 °C resulting in yellow plate crystals (0.41 g) forming over several days. These crystals were used for single crystal XRD and a yellow crystalline solid (2.82 g, 67%) was isolated from the remaining solution. Elemental analysis: calc. (found) (%) for $(NH_4)_{11}[Sm^{III}(PMo_{11}O_{39})_2]\cdot 26.0H_2O$: H 2.26 (2.10), N 3.63 (3.90), P 1.46 (1.74), Sm 3.55 (4.38), Mo 51.82 (52.20).

$(NH_4)_{11}[Dy(PMo_{11}O_{39})_2]\cdot xH_2O$ (3). This was synthesised as for **2** using $Dy(NO_3)_3\cdot 6H_2O$ (0.457 g, 1.0 mmol) to give a Dy : P stoichiometry of 1 : 2. Yellow plate crystals (0.32 g) formed over several days of storage of a portion of the preparative solution at 5 °C. These crystals were used for single crystal XRD and a yellow crystalline solid (2.78 g, 66%) was isolated from the remaining solution. Elemental analysis: calc. (found) (%) for $(NH_4)_{11}[Dy^{III}(PMo_{11}O_{39})_2]\cdot 22.4H_2O$: H 2.12 (1.97), N 3.68 (3.80), P 1.48 (1.84), Dy 3.88 (3.75), Mo 50.37 (50.55).

$(NH_4)_{11}[Lu(PMo_{11}O_{39})_2]\cdot xH_2O$ (4). This was synthesised as for **1** using $Lu(NO_3)_3\cdot 6H_2O$ (0.469 g, 1.0 mmol) to give a Lu : P stoichiometry of 1 : 2. Yellow plate crystals (3.31 g, 78% yield) formed over several days of storage of the preparative solution at 5 °C. A suitable crystal was used for single crystal XRD and the remaining material used for supporting analysis. Elemental analysis: calc. (found) (%) for $(NH_4)_{11}[Lu^{III}(PMo_{11}O_{39})_2]\cdot 24.5H_2O$: H 2.19 (2.03), N 3.64 (3.65), P 1.46 (1.59), Lu 4.13 (3.94), Mo 49.85 (50.35).

Crystallographic studies[22]

$(NH_4)_{11}[Ce(PMo_{11}O_{39})_2]\cdot 16H_2O$ (1). $H_{76}CeMo_{22}N_{11}O_{94}P_2$, M_r = 4047.46, monoclinic, space group $C2/c$, a = 38.035(10), b = 13.106(10), c = 19.840(10) Å, β = 117.70(3)°, V = 8756(8) Å^3, Z = 4, μ = 3.711 mm^{-1}, T = 293(2) K, cell parameters from 64729 reflections, θ = 1.67–26.37°, 8441 independent reflections, refinement was on F^2, $wR(F^2)$ = 0.0866, $R(F)$ = 0.0299. The crystal was mounted in a sealed capillary to prevent loss of solvent of crystallisation. The data were collected using the RAXIS in 127 × 2° phi oscillations of 10 min per exposure. The structure was solved by Patterson methods, and the asymmetric unit consists of half the molecule, with the Ce on a two-fold axis, together with solvent and cation sites. The NH_4 cations and solvent water molecules could not be distinguished, so 5.5 atoms with higher temperature factors were defined as N, and the remaining sites were assumed to be water. One of the water molecules was disordered over two sites at 0.5 occupancy each. H atoms were not included. The non-H atoms were refined anisotropically.

$(NH_4)_{11}[Sm(PMo_{11}O_{39})_2]\cdot 16H_2O$ (2). $H_{76}Mo_{22}N_{11}O_{94}P_2Sm$, M_r = 4057.69, monoclinic, space group $C2/c$, a = 38.00(3), b = 13.105(10), c = 19.915(10) Å, β = 117.77(3)°, V = 8774(11) Å^3, Z = 4, μ = 3,854 mm^{-1}, T = 293(2) K, cell parameters from

75760 reflections, $\theta = 1.67–25.02°$, 6900 independent reflections, $wR(F^2) = 0.2258$, $R(F) = 0.0760$. Data collected and structure solved as for **1**. Crystals were clearly twinned so the refinement for **1** was used as a starting point for the refinement of **2** as they were isomorphous with **1**. Twinning, and the high mosaic spread of the crystal, gave higher R values than for the isomorphous structures in **1**, **3** and **4**.

$(NH_4)_{11}[Dy(PMo_{11}O_{39})_2]\cdot 16H_2O$ (3). $H_{76}DyMo_{22}N_{11}O_{94}P_2$, $M_r = 4069.84$, monoclinic, space group $C2/c$, $a = 37.75(2)$, $b = 13.084(10)$, $c = 19.804(10)$ Å, $\beta = 117.54(3)°$, $V = 8673(9)$ Å^3, $Z = 4$, $\mu = 4.083$ mm^{-1}, $T = 293(2)$ K, cell parameters from 51893 reflections, $\theta = 1.22–25.03°$, 7434 independent reflections, $wR(F^2) = 0.0747$, $R(F) = 0.0273$. Data collection and structure solved as for **1**.

$(NH_4)_{11}[Lu(PMo_{11}O_{39})_2]\cdot 16H_2O$ (4). $H_{76}LuMo_{22}N_{11}O_{94}P_2$, $M_r = 4082.31$, monoclinic, space group $C2/c$, $a = 37.75(2)$, $b = 13.074(10)$, $c = 19.735(10)$ Å, $\beta = 117.40(4)°$, $V = 8603(8)$ Å^3, $Z = 4$, $\mu = 4.396$ mm^{-1}, $T = 293(2)$ K, cell parameters from 52624 reflections, $\theta = 1.67–25.02°$, 7134 independent reflections, $wR(F^2) = 0.0938$, $R(F) = 0.0347$. Data collection and structure solved as for **1**. Again, as for **2**, the crystals were twinned.

CCDC reference numbers 180315–180317 and 204416.

See http://www.rsc.org/suppdata/dt/b3/b301995k/ for crystallographic data in CIF or other electronic format.

Conclusions

We have structurally characterised a series of Ln^{III} polyoxometalate compounds containing the $[PMo_{11}O_{39}]^{7-}$ anion, $(NH_4)_{11}[Ln(PMo_{11}O_{39})_2]\cdot 16H_2O$ where $Ln^{III} = Ce^{III}$, Sm^{III}, Dy^{III} and Lu^{III}. These complexes form an isomorphous series, for which two of the phosphomolybdate lacunary anions sandwich one Ln^{III} cation, with distorted square-antiprismatic geometry around the central lanthanide. These complexes represent a rare example of the crystallographic characterisation of the lacunary phosphomolybdate anion, $[PMo_{11}O_{39}]^{7-}$ acting as a ligand. There is a systematic decrease in Ln–O distances and increase in splitting of the ν_{P-O} modes across the Ln series. Vibrational, UV/vis/nIR absorption and ^{31}P NMR spectroscopies give evidence for the stability of $[Ln(PMo_{11}O_{39})_2]^{11-}$ in solution. We are currently exploring whether or not the Ln^{III} ions can stabilise the $[PMo_{11}O_{39}]^{7-}$ anion over a wide pH range and if analogous complexes can be formed for all the rare-earth trivalent cations.

Acknowledgements

We thank Dr Steve Richardson and Dr Tracy Ward at BNFL Sellafield for useful discussions and the EPSRC and BNFL for funding.

References

1 L. C. Baker and D. C. Glick, *Chem. Rev.*, 1998, **98**, 1; M. T. Pope, *Heteropoly and Isopoly Oxometalates*, Springer-Verlag, Berlin, 1983.
2 J. F. Keggin, *Nature (London)*, 1933, **131**, 908; H. D'Amour and R. Allmann, *Z. Kristallogr*, 1976, **143**, 1.
3 H. Ichida, A. Kobayashi and Y. Sasaki, *Acta Cryst. B*, 1980, **36**, 1382; R. Strandberg and B. Hedman, *Acta Crystallogr., Sect. B*, 1982, **38**, 773; C. Rocchiccioli-Deltcheff, M. Fournier, R. Franck and R. Thouvenot, *Inorg. Chem.*, 1983, **22**, 207.
4 L. Petterson, I. Anderson and L. Ö. Öhman, *Inorg. Chem.*, 1986, **25**, 4726.
5 L. E. Briand, G. M. Valle and H. J. Thomas, *J. Mater. Chem.*, 2002, **12**, 299.
6 L. A. Combs-Walker and C. L. Hill, *Inorg. Chem*, 1991, **30**, 4016.
7 S. Himeno, M. Hashimoto and T. Ueda, *Inorg. Chim. Acta*, 1999, **284**, 237.
8 A. Gaunt, I. May and D. Collison, *Inorg. Chem.*, in press.
9 N. Honma, K. Kusaka and T. Ozeki, *Chem. Commun.*, 2002, 2896.
10 A. B. Yusov and V. P. Shilov, *Radiokhimiya*, 1999, **41**, 3.
11 See for example; E. M. Limanski, M. Piepenbrink, E. Droste, K. Burgemeister and B. Krebs, *J. Cluster Sci.*, 2002, **13**, 369; G. Xue, J. Vaissermann and P. Gouzerh, *J. Cluster Sci.*, 2002, **13**, 409; R. C. Howell, F. G. Perez, S. Jain, W. Dew. Horrocks, Jr., A. L. Rheingold and L. C. Francesconi, *Angew. Chem., Int. Ed.*, 2001, **40**, 4031; Q. Luo, R. C. Howell, J. Bartis, M. Dankova, W. Dew. Horrocks, Jr., A. L. Rheingold and L. C. Francesconi, *Inorg. Chem.*, 2002, **40**, 1894; K. Wasserman and M. T. Pope, *Inorg. Chem.*, 2001, **40**, 2763; Q. H. Luo, R. C. Howell, M. Dankova, J. Bartis, C. W. Williams, W. Dew. Horrocks, Jr., V. G. Young Jr., A. L. Rheingold, L. C. Francesconi and M. R. Antonio, *Inorg. Chem.*, 2001, **40**, 1894; M. Sadakane, M. H. Dickman and M. T. Pope, *Inorg. Chem.*, 2001, **40**, 2715.
12 Z. G Xiao, O. L. Chen and C. Chen, *J. Fujian Teachers University (Nat. Sci.)*, 1986, **2**(3), 77.
13 Y. K. Shan, Z. X. Liu, Z. S. Jin and G. C Wei, *Acta Chim. Sinica*, 1992, **50**, 357.
14 Y. K. Shan, Z. X. Liu, E. B. Wang, Z. S. Jin, G. C. Wei and Y. S. Liu, *Jiegou Huaxue*, 1990, **9**(3), 159.
15 E. B. Wang, Y. K. Shan, Z. X. Xu, J. F Liu and B. J Zhang, *Acta Chim. Sinica*, 1991, **49**, 774.
16 Z. X. Liu, Y. K. Shan, E. B. Wang, Z. S. Jin, G. C. Wei and Y. S. Liu, *Chem. J. Chinese Univ.*, 1991, **12**(1), 1.
17 Program used to create Fig. 1(b): Diamond version 2.1e (Klaus Brandenburg, Copyright 1996–2001, Crystal Impact GbR).
18 C. W. Haigh, *Polyhedron*, 1995, **14**, 2871.
19 R. Strandberg, *Acta. Crystallogr., Sect. B*, 1977, **33**, 3090.
20 L. Bi, E. Wang, L. Xu and R. Huang, *Inorg. Chim. Acta.*, 2000, **305**, 163.
21 C. J. Clark and D. Hall, *Acta Crystallogr., Sect. B*, 1976, **32**, 1545.
22 Cell refinement: DENZO (Z. Otwinowski, 1988). Data reduction: DENZO (Z. Otwinowski, 1988). Program used to solve structure: DIRDIF92 PATTY (P. Beurskens, 1992). Program used to refine structure: SHELXL97 (G. M. Sheldrick, 1997).